

Mean Temperature Field Effect on Acoustic Mode Structure in Dump Combustors

A. M. Laverdant*

Office National d'Etudes et de Recherches Aérospatiales, Châtillon, France

and

T. Poinsot* and S. M. Candel†

Centre National de la Recherche Scientifique (CNRS), Châtenay-Malabry, France

The acoustic modes of a dump combustor are calculated in this paper with a finite element method for three different temperature fields determined experimentally. It is shown that the inhomogeneous temperature distribution affects the eigenfrequencies and modifies the acoustic pressure and velocity distributions corresponding to the various modes. It is suggested that such analysis may indicate why certain acoustic modes favor an unstable behavior of the combustor.

Nomenclature

| | |
|----------------------|--|
| c, c_R | = local and reference sound speed |
| $C_p \hat{K}$ | = specific heat of K^{th} species, $\left(C_p = \sum_{K=1}^N C_{pK}\right)$ |
| f_K | = specific body force of K^{th} species |
| h | = enthalpy of the mixture defined in Eq. (6) |
| $[K]$ | = stiffness global matrix |
| L_R | = reference length |
| $[M]$ | = mass global matrix |
| M_K | = molar mass of K^{th} species |
| N | = local index of refraction, $= c_R/c$ |
| Ne | = number of finite elements |
| p | = pressure of the mixture |
| q | = heat flux defined in Eq. (7) |
| R_0 | = universal perfect gas constant, |
| | $\left(R = R_0 \sum_{K=1}^N Y_K/M_K\right)$ |
| t | = time |
| T | = temperature of the mixture |
| v | = velocity of the mixture |
| v_K^D | = diffusion velocity of the K^{th} species |
| w_K | = mass rate of production of the K^{th} species per unit volume |
| x, y | = cartesian coordinates |
| Y_K | = mass fraction of the K^{th} species |
| γ | = ratio of specific heats |
| ξ, ζ | = dimensionless local coordinates |
| ρ | = specific mass of the mixture |
| τ | = viscous stress tensor |
| Φ, ϕ, ϕ_1 | = dissipation function, test function, and equivalence ratio |
| ω, Ω | = dimensional and dimensionless angular frequencies |
| ∇, ∇ | = gradient and divergence operators |
| $<, >, \{ \}$ | = line and column vector |

Subscript

$()_R$ = reference quantity

Superscript

$(-)$ = steady component

$(-)', (-)$ = temporal and spatial components of acoustic perturbation

I. Introduction

COMBUSTION instabilities occur in many practical systems. Such instabilities are known to enhance heat transfer rates at the combustor wall and produce vibrations of large amplitude. In extreme cases, important structural damage and loss of control of the propulsion system are observed. When such phenomena are encountered in the development of a system, the usual practice is to follow a process of trial and error with the objective of suppressing or at least reducing the instability.

One type of combustion instability, which involves acoustic coupling, has been extensively studied in the past thirty years by a large number of authors. Some important studies on the subject were conducted by Crocco,¹ Crocco and Cheng,² Rogers and Marble,³ Culick,⁴ Barrère and Williams,⁵ and Crocco.⁶ A broad review of combustion instabilities in liquid rocket engines is contained in a classical volume edited by Harrje and Reardon.⁷

Some recent low-frequency instability problems occurring in ramjets and afterburners have given rise to new analytical developments by, for example, Marble and Candel,⁸ Marble et al.,⁹ Subbaiah,¹⁰ and Le Chatelier and Candel.¹¹ Recent experiments by Keller et al.,¹² Bray et al.,¹³ Davis,¹⁴ and Moreau et al.,¹⁵ provide new information on the problem. Parallel to these studies authors, such as Culick and Rogers¹⁶ and Yang and Culick,¹⁷ have conducted low-frequency instability studies in ramjets.

According to Culick,⁴ high frequency instabilities, involving transverse modes of oscillations of the combustor, appear when the gain mechanisms (essentially the combustion), are stronger than the loss mechanisms (viscous effects, heat transfer, nozzle damping). An accurate analysis of the balance between gain and loss mechanisms requires the characterization of the acoustic modal structure involved in the process. It has been shown by Rogers and Marble³ that a precise knowledge of the modal structure is necessary to examine how acoustic oscillations may trigger the nonsteady combustion process.

Presented as Paper 85-1249 at the AIAA/SAE/ASME/ASEE 21st Joint Propulsion Conference, Monterey, CA, July 8-10, 1985; received Oct. 8, 1985; revision received Feb. 28, 1986. Copyright © American Institute of Aeronautics and Astronautics, Inc., 1986. All rights reserved.

*Research Scientist.

†Professor of Mechanical Engineering, Ecole Centrale des Arts et Manufactures (also with ONERA). Member AIAA.

To date, the modal structure has generally been determined under the assumption of constant temperature and sound speed in the combustor. However, axial changes in temperature have been taken into account in recent studies of low-frequency instability in ramjets by Clark,¹⁸ and Clark and Humphrey,¹⁹ and in premixed ducted flames by Moreau et al.¹⁵ Axial changes in temperature are also taken into account in studies of sound propagation in ducts and combustion cans by Prasad and Crocker,²⁰ Kapur et al.,²¹ and Cummings.²² El-Raheb and Wagner²³ have recently examined the influence of temperature inhomogeneities on the transverse mode structure for resonant axisymmetric cavities. Recent experimental results by Darabiha²⁴ indicate that diverse temperature fields may exist for different equivalence ratios in a given combustor. It is then logical to examine how these temperature distributions influence the higher mode structures. This analysis may indicate why certain modes trigger and enhance the nonsteady combustion process while others are less effective. A precise determination of the modal structure taking into account the temperature inhomogeneity is also useful in the experimental mode identification, and it may serve as a guide for the choice of suppression devices.

In Section II of this paper, a wave equation is established, describing acoustic perturbations in an inhomogeneous reactive medium. The acoustic modes, corresponding to the left-hand side of this equation may be determined with a finite element formulation, presented in Section III. The results obtained for the three mean temperature fields are described in Section IV and discussed in Section V.

II. Theoretical Formulation

The description of acoustic wave generation and propagation in an inhomogeneous reactive medium may be based on a wave equation, which will be developed in this section. It is of course possible to develop this equation in the absence of sources. Also, modal calculations performed here do not require the exact form of these source terms. However, a complete wave equation including these terms is derived. This allows direct modal expansions of the wave field in the presence of sources. Such representation are, in fact, quite useful in combustion instability studies.

The general equations for a chemically reactive mixture of N gaseous species and many alternative expressions, may be found in Barrère and Prud'homme,²⁵ Williams,²⁶ and Toong²⁷:

$$\frac{\partial \rho}{\partial t} + \nabla \cdot \rho \mathbf{v} = 0 \quad (1)$$

$$\frac{\partial}{\partial t} \rho Y_K + \nabla \cdot \rho Y_K (\mathbf{v} + \mathbf{v}_K^D) = w_K \quad (2)$$

$$\frac{\partial}{\partial t} \rho \mathbf{v} + \nabla \cdot (\rho \mathbf{v} \mathbf{v}) = -\nabla p + \nabla \cdot \boldsymbol{\tau} + \sum_{K=1}^N \rho f_K Y_K \quad (3)$$

$$\frac{\partial}{\partial t} \rho h + \nabla \cdot \rho h \mathbf{v} = -\nabla \cdot \mathbf{q} + \frac{dp}{dt} + \Phi + \sum_{K=1}^N \rho Y_K v_K^D \cdot \mathbf{f}_K \quad (4)$$

$$p = \rho R T, \text{ where } R = R_0 \sum_{K=1}^N Y_K / M_K \quad (5)$$

$$h = \sum_{K=1}^N h_K Y_K = \sum_{K=1}^N \left(h_K^R + \int_{T_R}^T C_{pK} dT \right) Y_K \quad (6)$$

This system, Eqs. (1-6), contains, respectively, the conservation equations of mass, the K^{th} chemical species, the momentum, the energy written in the enthalpy form, the equation of state, and the definition of the mixture enthalpy (the meaning of the different variables is given in the nomenclature at the beginning). The global conservation of mass

requires

$$\sum_{K=1}^N w_K = 0 \text{ and } \sum_{K=1}^N \rho Y_K v_K^D = 0$$

The enthalpy balance introduces the dissipation function Φ and a heat flux \mathbf{q} which, in the absence of radiation effect, take the following form:

$$\Phi = \boldsymbol{\tau} : \nabla \mathbf{v}; \quad \mathbf{q} = -\lambda \nabla T + \sum_{K=1}^N \rho Y_K h_K v_K^D \quad (7)$$

Simplification and arrangement may be introduced by neglecting specific body forces, \mathbf{f}_K , by introducing the material derivative, $d/dt = \partial/\partial t + \mathbf{v} \cdot \nabla$, and by deriving an equation for the temperature which results from a combination of the species and energy equations. The following system is obtained:

$$\frac{dp}{dt} + \rho \nabla \cdot \mathbf{v} = 0 \quad (8)$$

$$\rho \frac{d\mathbf{v}}{dt} = -\nabla p + \nabla \cdot \boldsymbol{\tau} \quad (9)$$

$$\rho C_p \frac{dT}{dt} = -\nabla \cdot \mathbf{q} + \frac{dp}{dt} + \Phi - \sum_{K=1}^N h_K w_K + \sum_{K=1}^N h_K \nabla \cdot \rho Y_K v_K^D \quad (10)$$

where

$$C_p = \sum_{K=1}^N C_{pK}$$

is the specific heat of the mixture.

The introduction of Eq. (7) for \mathbf{q} transforms Eq. (10) into

$$\rho C_p \frac{dT}{dt} = \nabla \cdot \lambda \nabla T + \frac{dp}{dt} + \Phi - \sum_{K=1}^N h_K w_K - \sum_{K=1}^N \rho Y_K v_K^D C_{pK} \cdot \nabla T \quad (11)$$

By dividing Eq. (11) by $C_p T$, using the equation of state [Eq. (5)], and combining this equation with the mass balance, one obtains

$$\frac{1}{\gamma} \frac{d}{dt} \ln p + \nabla \cdot \mathbf{v} = \frac{1}{\rho C_p T} \left[\nabla \cdot \lambda \nabla T + \Phi - \sum_{K=1}^N h_K w_K - \sum_{K=1}^N \rho Y_K v_K^D C_{pK} \nabla T \right] + \frac{d \ln R}{dt} \quad (12)$$

Equation (9) is now rewritten in the form

$$\frac{d\mathbf{v}}{dt} + \frac{c^2}{\gamma} \nabla \ln p = \frac{1}{\rho} \nabla \cdot \boldsymbol{\tau} \quad (13)$$

Equations (12) and (13) may be combined by taking the divergence of the latter and subtracting the material derivative of the former:

$$\begin{aligned} \nabla \cdot \left(\frac{c^2}{\gamma} \nabla \ln p - \frac{d}{dt} \left(\frac{1}{\gamma} \frac{d \ln p}{dt} \right) \right) &= \nabla \cdot \left(\rho^{-1} \nabla \cdot \boldsymbol{\tau} \right) \\ &- \frac{d}{dt} \left(\frac{1}{\rho C_p T} \right) \left[\nabla \cdot \lambda \nabla T + \Phi - \sum_{K=1}^N h_K w_K \right. \\ &\left. - \sum_{K=1}^N \rho Y_K v_K^D C_{pK} \cdot \nabla T \right] - \frac{d^2 \ln R}{dt^2} - \nabla \mathbf{v} : \nabla \mathbf{v} \end{aligned} \quad (14)$$

This wave equation is similar to the expression established by Phillips²⁸ in a classical analysis of the aerodynamic generation of sound in nonreactive turbulent gas flows. Doak²⁹ and Kotake,³⁰ have suggested that this equation has an essential flaw because terms appearing in the right-hand side describe various features of the propagation of sound and should be included in the left-hand side. However, the terms appearing in the right-hand side of Eq. (14) shall be regarded as source terms generating pressure waves in the reactive mixture. An analysis of the order of magnitude of each source term by Kotake³⁰ shows that the dominant mechanisms are the chemical heat release fluctuations and velocity perturbations. Neglecting all other terms, we obtain

$$\nabla \cdot \frac{c^2}{\gamma} \nabla \ln p - \frac{d}{dt} \left[\frac{1}{\gamma} \frac{d}{dt} \ln p \right] = \frac{d}{dt} \left[\frac{1}{\rho C_p T} \sum_{K=1}^N h_K w_K \right] - \nabla \mathbf{v} : \nabla \mathbf{v} \quad (15)$$

For the dump combustor considered in this work, the low speed of the reactive flow permits us to neglect the convective term in the material derivative: $d/dt \approx \partial/\partial t$. It is also assumed that the specific heat ratio is constant. Equation (15) then becomes

$$\nabla \cdot c^2 \nabla \ln p - \frac{\partial^2}{\partial t^2} \ln p = \frac{\partial}{\partial t} \left[\frac{1}{\rho C_p T} \sum_{K=1}^N h_K w_K \right] - \gamma \nabla \mathbf{v} : \nabla \mathbf{v} \quad (16)$$

This last equation is not linearized and, therefore, may be used to describe finite amplitude waves. However, in many circumstances, the pressure waves are relatively weak, and linearization is, therefore, possible. The pressure may then be expressed as a sum of a mean and a fluctuating component: $p = \bar{p} + p'$, with $|p'|/\bar{p}| \ll 1$. Then $\ln p \approx p'/\bar{p}$. In most practical combustors, the mean pressure does not change by more than a few percent, and the spatial derivative of \bar{p} may be neglected. This yields

$$\nabla \cdot c^2 \nabla p' - \frac{\partial^2 p'}{\partial t^2} = \frac{\partial}{\partial t} \left[(\gamma - 1) \sum_{K=1}^N h_K w_K \right] - \gamma \bar{p} \nabla \mathbf{v} : \nabla \mathbf{v} \quad (17)$$

In addition to this equation, an expression for the acoustic velocity is needed. This is obtained by linearization of the momentum equation, Eq. (13), and by neglecting the viscous stresses. This gives

$$\frac{\partial \mathbf{v}'}{\partial t} = -\bar{p}^{-1} \nabla p' \quad (18)$$

Equations (17) and (18) describe the propagation and generation of small perturbations in a reactive mixture.

To perform a modal analysis, it is first assumed that all waves are harmonic and contain the common factor $\exp(-i\omega t)$. The modes are the eigensolutions of the Helmholtz equation for an inhomogeneous medium

$$\nabla \cdot c^2 \nabla \bar{p} + \omega^2 \bar{p} = 0 \quad (19)$$

and the corresponding velocity is described by

$$\bar{\mathbf{v}} = (\rho i \omega)^{-1} \nabla \bar{p} \quad (20)$$

These equations must be solved under the usual boundary conditions:

$$\bar{\mathbf{v}} \cdot \mathbf{n} = 0, \text{ on a rigid wall; and } \bar{p} = 0, \text{ plane exit} \quad (21)$$

This set of equations is nondimensionalized by introducing the following reduced variables and operators:

$$\nabla_* = L_R \nabla; \bar{p}_* = \bar{p}/\gamma p_R; \mathbf{v}_* = \bar{\mathbf{v}}/c_R; \Omega = \omega L_R/c_R; N^2 = c_R^2/c^2 \quad (22)$$

With these definitions, Eqs. (19) and (20) become

$$\nabla_* \cdot (N^{-2} \nabla_* \bar{p}_*) + \Omega^2 \bar{p}_* = 0 \quad (23)$$

$$\bar{\mathbf{v}}_* = (N^2 i \Omega)^{-1} \nabla_* \bar{p}_* \quad (24)$$

All variables are now dimensionless, and it is possible to omit the (*) and (̄) symbols in the following developments.

III. Finite Element Formulation

The combustor under study is rectangular with a square cross section. The mean flow is nearly two dimensional and this property also characterizes the main modes of oscillations. Then, it is natural to use a two dimensional finite element formulation of the Galerkin type^{31,32} to solve the problem.

A test function ϕ which satisfies the boundary conditions [Eq. (21)] is now introduced. Equation (23) is multiplied by ϕ and integrating over the surface of the cavity, this gives

$$\int_S \nabla \cdot (N^{-2} \nabla p) \phi dS + \Omega^2 \int_S \phi p dS = 0 \quad (25)$$

The first integral may be replaced by

$$\int_S \nabla \cdot (N^{-2} \nabla p) \phi dS = \int_S \nabla \cdot (\phi N^{-2} \nabla p) dS - \int_S N^{-2} \nabla p \cdot \nabla \phi dS \quad (26)$$

Using Green's theorem and the boundary conditions on ϕ and p , it is easy to show that the first term of the right-hand side of Eq. (26) vanishes. Equation (25) then becomes

$$- \int_S N^{-2} \nabla p \cdot \nabla \phi dS + \Omega^2 \int_S \phi p dS = 0 \quad (27)$$

The combustor is subdivided into N_e triangular elements. The variation of the pressure within each element is approximated with a linear polynomial

$$p = ax + by + c = a_1 \xi + b_1 \zeta + c_1 = \langle Q_1 \rangle \cdot \{p_n\} \quad (28)$$

x, y are the cartesian coordinates for a triangular element, while ξ, ζ are dimensionless local coordinates of a reference triangular element:

$$x = \sum_{j=1}^3 Q_{1j}(\xi, \zeta) x_j, \quad y = \sum_{j=1}^3 Q_{2j}(\xi, \zeta) y_j \quad (29)$$

The introduction of Eqs. (28) and (29) into Eq. (27) yields

$$\sum_{e=1}^{N_e} \left[\langle \delta p_n \rangle \left(\int_{S_e} N^{-2} \langle \nabla Q_1 \rangle \cdot (\nabla Q_1) \{p_n\} dS \right) - \langle \delta p_n \rangle \Omega^2 \int_{S_e} \langle Q_1 \rangle \cdot Q_1 \{p_n\} dS \right] = 0 \quad (30)$$

After a reformulation, this equation is presented as an eigenvalue problem:

$$[K] - \Omega^2 [M] = [0]$$

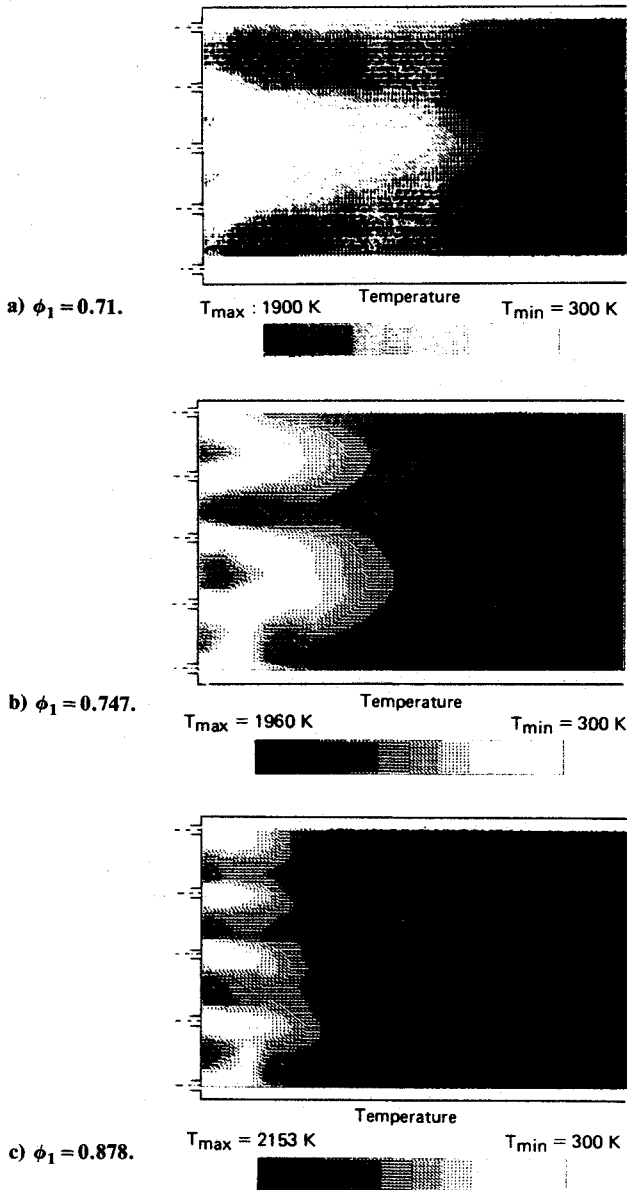


Fig. 1 Temperature distribution in the dump combustor deduced from gas measurements. The inlet plane is shown on the left of the figure.

where

$$[K] = \sum_{e=1}^{Ne} [K_e] = \sum_{e=1}^{Ne} \int_{S_e} N^{-2} \langle \nabla Q_1 \rangle \cdot \nabla Q_1 dS$$

$$[M] = \sum_{e=1}^{Ne} [M_e] = \sum_{e=1}^{Ne} \int_{S_e} \langle Q_1 \rangle \cdot \{Q_1\} dS \quad (31)$$

The stiffness and mass global matrices $[K]$ and $[M]$ are formed by assembling the elementary matrices $[K_e]$ and $[M_e]$, which relate to a single triangular element of surface S_e .

The eigenvalues Ω corresponding to each acoustic mode may be evaluated with a Jacobi algorithm. The pressure gradient components and the amplitude of acoustic velocity are then evaluated.

IV. Numerical Results

To compare the modes of the combustor, three mean temperature fields, determined experimentally from gas

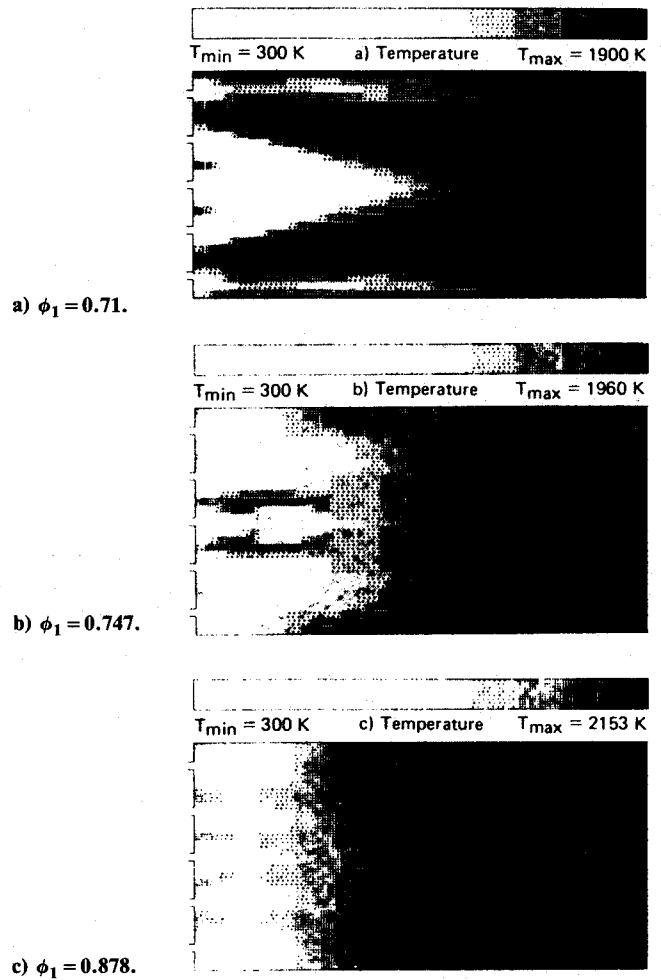


Fig. 2 Discretized temperature field distribution in the dump combustor.

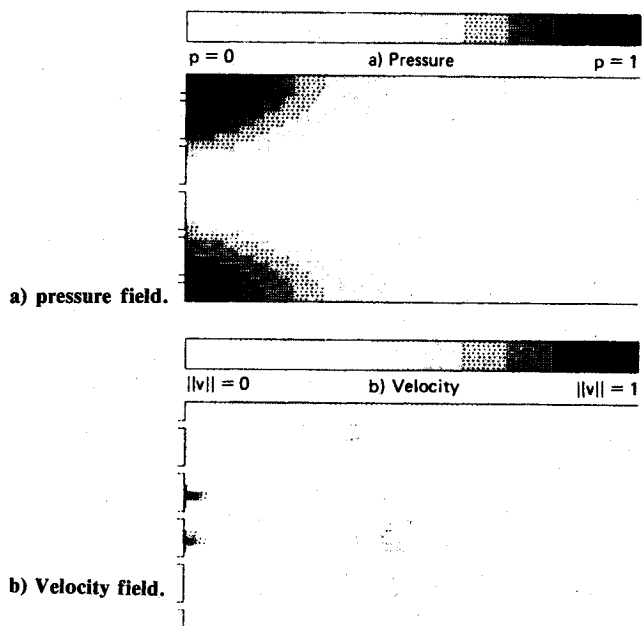
analysis measurements,²⁴ are presented for three mass flow rates and equivalence ratio in Fig. 1a-c. The mean field presented on Fig. 1 corresponds to $\phi_1 = 0.71$. The periodicity at the injection plane does not persist downstream; the three inner jets strongly interact while the two outer jets are deflected toward the walls. Combustion products recirculate behind the backward facing steps which separate the jets in the injection plane. For an equivalence ratio of $\phi_1 = 0.747$ (Fig. 1b), the jets are interacting by groups of two, while the lower jet is isolated. For $\phi_1 = 0.878$, the jets remain separated downstream (Fig. 1c).

To calculate the eigenmodes, it is necessary to idealize the experimental temperature fields. For computational simplicity, the three fields are symmetrized. In addition, the gas analysis measurements cannot be performed near the walls and the temperature is extrapolated in these regions. The discretized temperature fields are displayed in Fig. 2a-c. An examination of the experimental and idealized temperature fields shows differences which could be due to an imperfect discretization and the grey scale used for this representation. These input data are then used to calculate the local refraction index: $N = c_R / (\gamma RT)^{1/2}$ where $c_R = 344$ m/s is a reference sound speed (the sound speed of an air-propane mixture for $\phi_{1R} = 0.8$ and $T_R = 300$ K). The reference length retained in the calculations is the height of the combustor $L_R = h = 0.1$ m.

The eigenfrequencies corresponding to the first four eigenmodes and the three equivalence ratios are presented in Table 1. The structure of a single mode (1T-1L) for the three equivalence ratios shall now be examined.

Table 1 Eigenfrequencies of the four first modes for three equivalence ratios

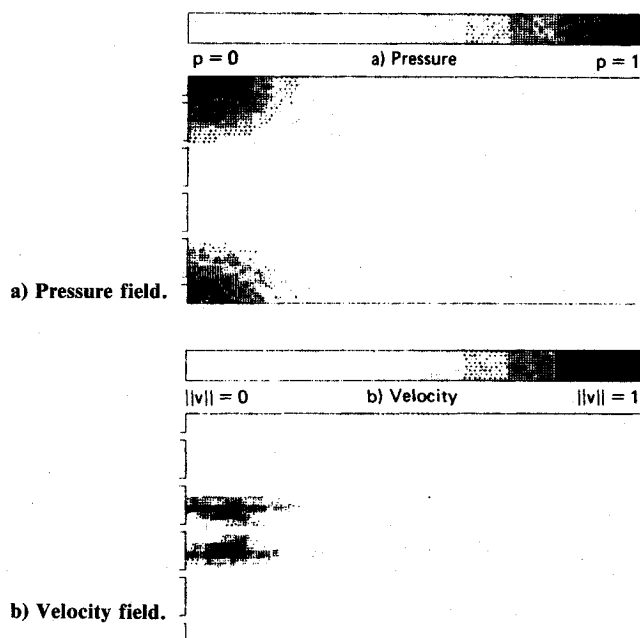
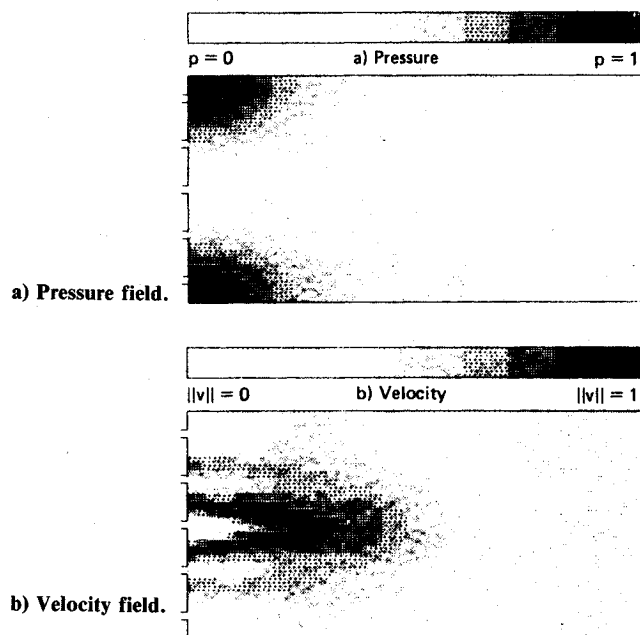
| f, Hz | Modes | | | |
|------------------|-------|------|-------|------|
| | 1L | 2L | 1T-1L | 3L |
| $\phi_1 = 0.71$ | 789 | 2643 | 3528 | 4539 |
| $\phi_1 = 0.747$ | 750 | 2540 | 2772 | 4352 |
| $\phi_1 = 0.878$ | 896 | 2932 | 3453 | 5063 |

**Fig. 3** Pressure and acoustic velocity amplitude distributions for the 1T-1L mode and $\phi_1 = 0.71$.

The pressure and acoustic velocity fields are displayed on a scale of grey levels in Figs. 3-5. For the lowest equivalence ratio $\phi_1 = 0.71$, the pressure amplitude distribution (Fig. 3a) is qualitatively close to that of a 1T-1L mode for at homogeneous sound speed field under the same boundary conditions. The acoustic velocity amplitude is displayed in Fig. 3b. It exhibits strong variations due to the large changes in local index. Two velocity antinodes are located near the injection plane and large gradients may be observed in the reaction zone. An examination of the two other modal structures shows that the pressure amplitude contours have the same general shape. However, their spatial location changes with the equivalence ratio. The acoustic velocity distributions change even more drastically, and they strongly depend on the local index values. The velocity amplitude reaches large values near the inlet plane in the reactive zone. Phase information for the pressure is not displayed here because in eigenmode calculations the phase takes values of 0 and π depending on the pressure sign. Thus, the phase may be easily deduced from the plots of Fig. 3 by nodal line location.

V. Discussion

These calculations provide new information on eigenfrequencies and modal structures for a simplified dump combustor. It is found that the eigenfrequencies do not change monotonically with the equivalence ratio. The variation depends on the maximum temperature reached by the mixture, but the flame structure is also influential. Hence, the simplified prediction that the eigenfrequencies are proportional to the square root of T fails. This statement is valid for a homogeneous temperature field, but is not adequate if

**Fig. 4** Pressure and acoustic velocity amplitude distributions for the 1T-1L mode and $\phi_1 = 0.747$.**Fig. 5** Pressure and acoustic velocity amplitude distributions for the 1T-1L mode and $\phi_1 = 0.878$.

there are changes in temperature distribution in the combustor.

The pressure amplitude corresponding to a given mode is also affected by the temperature field. The acoustic velocity strongly differs from the homogeneous case. The velocity amplitude reaches large values in regions where the temperature has a strong gradient (reaction zones). Concerning the acoustically coupled combustion instabilities, this may explain why certain modes are easier to trigger than others.

Acknowledgments

Part of this work has been performed under contract from DRET at ONERA and Ecole Centrale. The authors wish to

thank Drs. Paul Kuentzmann, Roland Borghi and Frank Marble for helpful discussions and Dr. Darabiha for providing the temperature maps.

References

- ¹Crocco, L., "Research on Combustion Instability in Liquid Rocket," *Twelfth Symposium (International) on Combustion*, The Combustion Institute, Pittsburgh, PA, 1968, pp. 85 and 99.
- ²Crocco, L. and Cheng, S. I., "Theory of Combustion Instability in Liquid Propellant Rocket Motors," AGARDograph No. 8, Butterworths, London, 1956.
- ³Rogers, D. E. and Marble, F. E., "A Mechanism for High Frequency Oscillations in Ramjet Combustors and After Burner," *Jet Propulsion*, Vol. 26, June 1956, p. 456.
- ⁴Culick, F. E. C., "Stability of High Frequency Pressure Oscillations in Rocket Combustion Chambers," *AIAA Journal*, Vol. 1, May 1963, pp. 1097 and 1104.
- ⁵Barrere, M. and Williams, F. A., "Comparison of Combustion Instabilities Found in Various Type of Combustion Chambers," *Twelfth Symposium (International) on Combustion*, The Combustion Institute, Pittsburgh, PA, 1968, pp. 169 and 181.
- ⁶Crocco, L., "Theoretical Studies on Liquid-Propellant Rocket Instability," *Tenth Symposium (International) on Combustion*, The Combustion Institute, Pittsburgh, PA, 1965, pp. 1101 and 1128.
- ⁷Harje, D. T. and Reardon, F. H. (eds.), *Liquid Propellant Rocket Combustion Instability*, NASA SP-194, 1972.
- ⁸Marble, F. E. and Candel, S. M., "An Analytical Study of the Non Steady Behavior of Large Combustor," *Seventeenth Symposium (International) on Combustion*, The Combustion Institute, Pittsburgh, PA, 1978, pp. 761 and 769.
- ⁹Marble, F. E., Subbaiah, M. V., and Candel, S. M., "Analysis of Low Frequency Disturbances in Afterburners," *Proceedings of Specialists Meeting on Combustion Modeling*, AGARD Propulsion and Energy Panel, Cologne, FRG, AGARD CP275, 1979.
- ¹⁰Subbaiah, M. V., "Non Steady Flame Spreading in Two Dimensional Ducts," *AIAA Journal*, Vol. 21, Nov. 1983, pp. 1557 and 1564.
- ¹¹Le Chatelier, C. and Candel, S. M., "Flame Spreading in Compressible Duct Flow," *Proceedings of the First Specialists Meeting of the Combustion Institute*, Bordeaux, France, 1981.
- ¹²Keller, J. O., Vaneveld, L., Korschelt, D., Ghoneim, A. F., Daily, J. W., and Oppenheim, A. K., "Mechanism of Instabilities in Turbulent Combustion Leading to Flashback," *AIAA Journal*, Vol. 20, Feb. 1982, pp. 254 and 262.
- ¹³Bray, K. N. C., Campbell, I. G., Lee, O. K., and Moss, J. B., "An Investigation of Reheat Buzz Instabilities," *Aeronautics and Astronautics*, University of Southampton, England, AASU Memo 83/2, 1983.
- ¹⁴Davis, D. L., "Coaxial Dump Combustor Combustion Instabilities—Part I—Parametric Test Data," APL, AFWAL, Interim Rept., Wright Patterson AFB, OH, 1981.
- ¹⁵Moreau, P., Candel, S. M., Piquemal, J. M., and Borghi, R., "Phénomène d'Instabilité dans un Foyer Turbulent," *Proceedings of the First International Specialists Meeting of the Combustion Institute*, Bordeaux, France, 1981.
- ¹⁶Culick, F. E. C. and Rogers, T., "The Response of Normal Shocks in Diffusers," *AIAA Journal*, Vol. 21, Oct. 1983.
- ¹⁷Yang, V. and Culick, F. E. C., "Linear Theory of Pressure Oscillations in Liquid Fuel Ramjet Engines," AIAA Paper 83-0574, Jan. 1983.
- ¹⁸Clark, W. H., "Experimental Investigation of Pressure Oscillations in a Side Dump Ramjet Combustor," *Journal of Spacecraft and Rockets*, Vol. 19, Jan.-Feb. 1982, pp. 47 and 53.
- ¹⁹Clark, W. H. and Humphrey, J. W., "Identification of Longitudinal Acoustic Modes Associated with Pressure Oscillations in Ramjet," AIAA Paper 84-1405, June 1984.
- ²⁰Prasad, M. G. and Crocker, M. J., "Evaluation of a Four Pole Parameter for a Straight Pipe with a Mean Flow and a Linear Temperature Gradient," *Journal of the Acoustical Society of America*, Vol. 69, No. 4, April 1981, pp. 916 and 921.
- ²¹Kapur, A. et al., "Sound Propagation in a Combustion Can with Axial Temperature and Density Gradients," *Journal of Sound and Vibration*, Vol. 25, No. 1, Nov. 1972, p. 129 and 138.
- ²²Cummings, A., "Ducts with Axial Temperature Gradients: An Approximate Solution for Sound Transmission and Generation," *Journal of Sound and Vibration*, Vol. 51, No. 1, March 1977, pp. 55 and 67.
- ²³El-Raheb, M. and Wagner, P., "Acoustic Propagation in Resonant Axisymmetric Cavities Enclosing an Inhomogeneous Medium—Part I—Hollow Cavity," *Journal of the Acoustical Society of America*, Vol. 74, No. 5, Nov. 1983, pp. 1583 and 1596.
- ²⁴Darabiha, N., "Un Modèle de flamme cohérente pour la combustion prémélangée: Analyse d'un Foyer Turbulent à Elargissement Brusque," Ph.D. Thesis, Ecole Centrale des Arts et Manufactures, Châtenay-Malabry, France, 1984.
- ²⁵Barrère, M. and Prud'homme, R., *Equations Fondamentales de l'Aérodynamisme*, Masson, Paris, France, 1973.
- ²⁶Williams, F. A., *Combustion Theory*, Addison Wesley, 1965.
- ²⁷Toong, T. Y., *Combustion Dynamics*, McGraw Hill, New York, 1983.
- ²⁸Phillips, O. M., "On the Generation of Sound by Supersonic Turbulent Shear Layers," *Journal of Fluid Mechanics*, Vol. 9, 1960, pp. 1 and 28.
- ²⁹Doak, P. E., "Fundamentals of Aerodynamic Sound Theory and Flow Duct Acoustics," *Journal of Sound and Vibration*, Vol. 28, 1973, pp. 527 and 561.
- ³⁰Kotake, S., "On Combustion Noise Related to Chemical Reactions," *Journal of Sound and Vibration*, Vol. 42, 1975, pp. 399 and 410.
- ³¹Zienkiewicz, O. C., *The Finite Element Method*, McGraw Hill, New York, 1977.
- ³²Dhatt, G. and Touzot, G., *Une présentation de la Méthode des éléments finis*, Maloine, Paris, France, 1981.